

Brain Abnormality Categorization

Anshumaan Phukan¹, Adarsh Raghav², Varad Vinayak Godse³

^{1,2,3} Dept. of Computer Science Engineering, Bennett University, Greater Noida, Uttar Pradesh, India

Abstract - In the past decade, developments in the field of medical analysis and imagery have been exponential. Logical approaches to intricate problems have played a significant role in the larger picture: medical diagnosis and treatment. This paper discusses the detection of brain abnormalities, casualties, and complex analysis of medical imagery such as Magnetic Resonance Images and X-rays in a more focused spectrum. The most common occurring brain disorders today stem from brain abnormalities. The general practice is to have a neurologist analyze many patient images, which becomes extremely tedious and inefficient. In this work, we propose an abnormality detection workflow revolving around advanced machine learning techniques to study the brain's medical images (X-rays/MRIs).

With more than 700 unlabeled patient images, we would label and pre-process these images (resizing, orientation, grayscale, and noise removal). Then, further classifying the images into 'brain' and 'not brain' using a neural network-based classifier framework. With these concrete brain images and a convoluted neural network architecture, we will classify the brain images; 'Normal' and 'Abnormal.' These predictions will be based on the learning from training data. The further steps in classification include modifications to improve accuracies and training on larger datasets to get a better fit.

1. INTRODUCTION

1.1 PROBLEM AND MOTIVATION

According to a 2007 study organised by the United Nations, up to 1 billion people suffer from one form of a neurological disorder or the other. To expand, these disorders/abnormalities vary from something as severe as Alzheimer's disease to some as minute as a migraine.

A logical approach for diagnosing such abnormalities is to conduct an MRI (Magnetic Resonance Imaging) of the patient's brain followed by a short-sighted examination of these MRI/X-ray. Unfortunately, such a procedure can often be tedious and inefficient. As per standard protocols, the neurologist has to pace through multiple scans of a single brain to accurately determine the root cause and occurrence of abnormalities in most cases. Thus, such an approach can lead to inaccuracy, latency, and false positives.

1.2 BACKGROUND KNOWLEDGE

Before beginning our project, we had to construct ideation of our project. The ideation process encompassed various parameters to analyze and metricate our idea and the approach we were to take to reach the most optimal solution. Furthermore, since our idea is structured on medical imagery and analysis and, more specifically, neurology, the solution demanded in-depth research into brain abnormalities: what they are, how they are caused, and how they can be detected/treated.

In layman's terms, a brain tumor is a neurological anomaly that may occur due to the presence of atypical features in brain function. Now, this atypical feature can occur due to multiple causes such as:

- Damage to the brain through an accident or traumatic event (such as concussions/blood clots/ strokes)
- Parental Genetics
- Toxins/diseases that may have been passed on from the parent
- Some this can be caused by other diseases such as:
 - Epilepsy

- Malignant Tumors
- Scoliosis
- Parkinson's Disease
- Cancer/Infections

The next step is to understand how doctors process detecting and treating brain abnormalities. An initial approach is to get the patients' symptoms mapped, where initial symptoms can range from vomiting, nausea, speech difficulty, paralysis, and memory loss.

A more precise and well-adapted approach is to conduct a Magnetic Resonance Image (MRI) of the patient's brain, which returns an X-ray-like view of the patient's brain. The doctor can then use this MRI to detect malignant abnormalities in how the patient's brain is structured.

In fig 1 below, we can see the side-by-side comparison of 2 brain MRIs. The scan to the left is of a patient with no visible abnormalities, whereas the image to the right is of a brain abnormality.

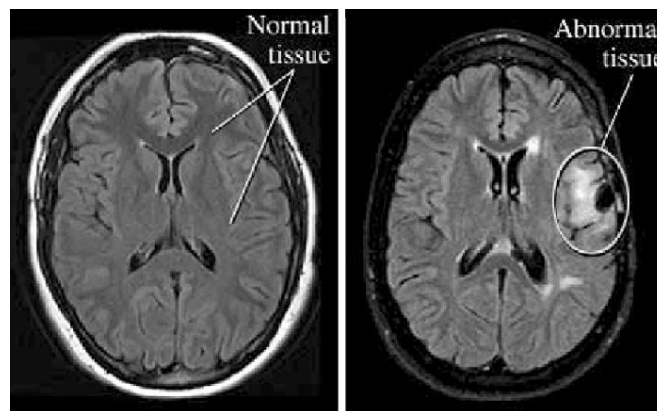


Fig. 1. Magnetic Resonance Image of 2 patients (one with normal brain and the other with an abnormal brain)

As seen in the scan to the right, the patient has abnormal tissue in the brain, which can be spotted as a white highlight towards the center of the scan. Unique patterns such as these can be used to detect any malignant in the brain, further helping us classify whether the brain is abnormal.

2. RELATED WORK

A. Related Work 1

While doing our research on this topic, we took heavy inspiration from a scientific journal where the researchers took anomaly detection approach to identify chronic brain infarcts on MRI. They discovered an effective approach to detect all anomalies by learning how 'normal' tissue looks using their anomaly detection technique. A total of 967 patients were enrolled in this study, with 270 of them suffering from brain infarctions. Before creating the model, they performed fundamental image preprocessing activities such as N4 bias field correction and normalization. For the required training dataset, 1 million transversal image patches (15*15 voxels) were sampled from images of all but 10 patients without brain infarcts. The neural network architecture they implemented was based on the GANomaly architecture which consisted of generator (bottom half) and discriminator (top half). The generator and discriminator they used consisted of encoder and decoder parts. Each parts contained three sequential convolutional layers, interleaved with Relu activation and batch normalization. Encoding of input image patches x into latent representations: z and \hat{z} were done using generator and creation of realistic reconstructions x^* was done using discriminator. Adam was used as the optimizer with a learning rate of 0.001.

Conclusion found in this paper:

- In comparison to all other latent vector sizes, a latent vector size of 100 had the maximum sensitivity and detected brain infarct volume percentage for the same number of suspected abnormalities over practically the full range, according to the validation set. On the test set, the suggested method yielded an average of 9 suspected abnormalities per image while using optimal parameters for evaluation. Their neural network detected 374 out of 553 brain infarcts (sensitivity: 68 percent).
- White matter hyper intensities were responsible for 44.3 percent (865) of the suspected abnormalities.
- Normal healthy tissue was shown to be responsible for 563, or 28.8%, of all detected abnormalities.
- The researchers discovered that 1.3 percent of all suspected anomalies were unannotated brain infarcts, which were typically located within the cerebellum.

B. Related Work 2

We also had great insight from another similar research paper. what they did was that they basically trained an autoencoder on a perfectly healthy brain's MRI images and went on with it to detect anomalies like glioblastoma, microangiopathy and multiple sclerosis.

They used this feature of spatial encoders, which by the way could flatten and refurbish the data so that they could learn more about the irregularity of a healthy brain given its MR images. They trained this unsupervised model with 100 normal, perfectly healthy MRI in-house scans. By making out the difference of input data and its revamping, with the help of this feature they could detect and delineate several diseases. The model was held in contrast with a supervised UNet and other models based on threshold, which were trained with images of total of hundred patients MR scan images, fifty patients suffering with sclerosis (multiple), which was an autogenous dataset, and another fifty patients out of CIA (Cancer Imaging Archive). Thereafter, both the UNet models were tested with 5 datasets of different brain abnormalities like glioblastoma, microangiopathy and multiple sclerosis. UNet is a basically a neural network architecture extension features with some editions in the CNN architecture, to deal with biomedical images where the goal is to find the area of the infection along with the affirmation of an anomaly.

Conclusion found in this paper:

They used precision-recall statistics like F1 Score, Dice Score, mean area under the curve and etc. to facilitate segmentation performance. The unsupervised method won over the thresholding model in various aspects. An anomaly heatmap display was created of the model. The unsupervised model showed a F1 Score of 17% to 62% for tumour identification. The naïve thresholding model was tested across five datasets, revealing them a 6.4%-15% F1 Score. The UNet Model (supervised) meanwhile came close to the unsupervised model with a F1 score ranging in the region of 20% to 40%. With a mean precision score of 15%-59%, the unsupervised models had an upper hand over the thresholding models, which has 3.4%-10% MP score. This vast difference of mean precision score credited to the unsupervised model's success. After gathering all the data, they came up with a conclusion that Deep Learning Unsupervised Model would identify more potential abnormalities efficiently from a given input MRI scan image of the brain.

3. INTRODUCTION

Previous Approach

The image data comes in Dicom format (.dic extension). Every image gets converted to JPEG through rescaling. The prepared JPEG data needs manual labelling at the beginning. The images get labeled as brain or not brain. The labeled dataset moves into the binary classifier for training. The CNN model classifies the image as "BRAIN" or "NOT BRAIN" based on the learning from training data. The further steps in classification include modifications to improve accuracies.

The image detection process needs detailed annotated images for training. The different parts of brain images must be annotated in required forms like bounding boxes, polygons, etc. The dimensions of annotated parts get stored in txt formats like XML. The dimension data on every image can then move for training. The neural network for object detection trains itself and detects the different parts of the brain image.

The abnormalities in a brain image require the analysis of specific brain parts. The features of the identified parts get compared to conditions that fulfil an abnormal image. The images get labeled as Abnormal and Normal. The labeled dataset moves into the binary classifier for training. The CNN model classifies the image as "ABNORMAL" or "NORMAL" based on the learning from training data. The further steps in classification include modifications to improve accuracies.

New Approach

The first approach included detecting the brain parts and applying conditions to classify them as 'Abnormal' or 'Normal'. It is computationally possible, but the chances of errors are more. The nature of the annotations included complex edge and polygon selection, and minor errors could have led to inaccurate results. The degree of randomness of the abnormality on brain images would have generated the need for a large number of annotated samples. The comparison process would have been tedious because no preexisting models are working on a similar approach.

The second approach functions through the traditional binary classification process. It trains the model with a labeled dataset which in turn predicts the two classes. The nature of the approach makes comparison easy as many models share a similar structure. It leads to faster improvements, better insights, and accuracies.

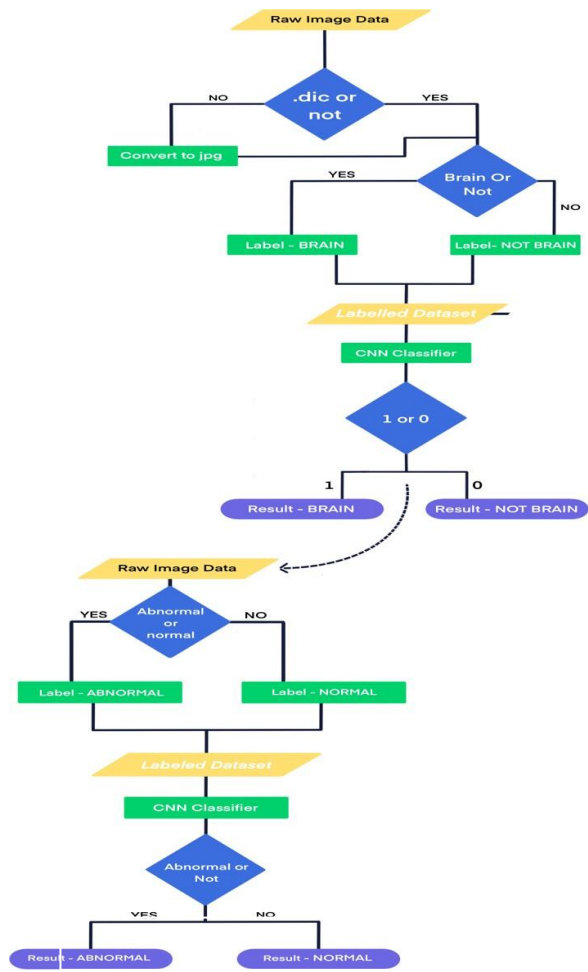


Fig2. Methodology flowchart

3. PROPOSED METHODOLOGY

The Data

The initial image data consisted of random MRI images belonging to multiple categories. It included the spine, bladder, and brain. The brain images corresponded to three sub-parts, namely T1W, T2W, and flair. The majority portion of T1W images is bright with dark ventricles. The T2W is dark with bright ventricles, while the flair has a slightly bright greyish portion with dark ventricles. The classification of a particular category needs at least one other differentiation against it. The image data had around 720 images of the brain (T1W, T2W, Flair), spine, gall bladder. The number of samples from each category was unknown. The classification needed T1W, T2W, and flair images from the two categories (ABNORMAL and NORMAL). The dataset had 400 images with an unknown number of samples from each class. MRI: an imaging technique that uses magnets (magnetic field) and radio waves to create images of inner parts of the body. A CT uses X-rays to do the same function.

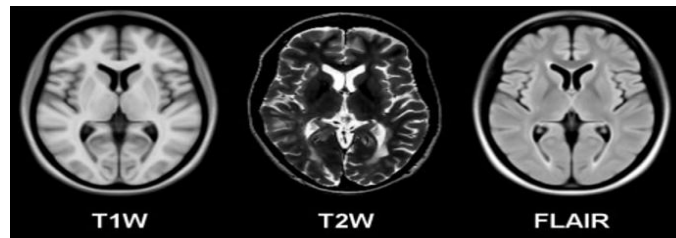


Fig. 3. Magnetic Resonance Image of the brain

A. Labelling

The images needed manual labelling or categorizing. The Pigeon Jupyter library of python helps to achieve the task. The `annotate` function under the library inputs the folder path and the labels to be assigned. It traverses every image and asks the user to categorize accordingly.

The dataset consisting of 720 images went through `annotate` function to get labeled as BRAIN and NOT BRAIN. The function returns a NumPy array with image paths and labels at the end. The training phase makes use of it later. The dataset (NORMAL and ABNORMAL) having 400 images followed the same annotating steps.

B. Pre-Processing

The image dataset came in the form of image paths along with labels. The classification model does not understand string paths or images. The conversion to numerical form is necessary. The `IMAGE` function under the PIL library of python helps to open the image. It provides read and writes operations on the file. The `ASARRAY` function from the NumPy library further converts them into arrays. The data used for both the classification came in different configurations. It was a random collection of grayscale and RGB channel pictures. The numerical difference lies in the shape of NumPy arrays of the images.

For example, a grayscale image array shape would be $\rightarrow (256,300)$. It means that the array is two-dimensional with an outer size of 256 and each of the 256 blocks has 300-pixel values. The pixel values represent the degree of brightness that ranges from 0-255, with zero representing the darkest value and 255 as the brightest.

An RGB image array shape would be $\rightarrow (256,300,3)$. It means that the array is three-dimensional with an outer size of 256. The size of the second layer is 300, with each block having 3-pixel values. The pixel-values represent distribution over RGB (Red, Green, Blue).

The images came in different sizes like $(256,330)$ or $(400,1000)$. However, the architecture of a neural network needs to be defined based on the input size. The different sizes in every iteration can cause errors; hence, the image arrays have to resize similarly. The "resize" function from the CV2 library or "np. resize" function from the NumPy library carries out the task properly.


The image data is ready for training after these steps. Other techniques we used for image processing were:

- a. , it has the added feature of evaluating pixel density. It contains two notable features:
- b. Median blurring: While applying convolution to the full image, this pre-processing activity takes the median of all the pixels in the kernel area and replaces the core element with the median value. This approach is very good at reducing salt and papernoise from MRI scans, which can be rather prevalent.
 - Bilateral Filtering: This approach is mostly used to remove noise while keeping edges intact. In comparison to other blurring algorithms Gaussian function of space: Only pixels in closeproximity are examined
 - Gaussian function of intensity: only pixels with similarintensities are examined

It ensures that only pixels with matching intensity values to the core pixel are evaluated for blurring, while maintaining sharp intensity changes.

$$BF[I]_p = \frac{1}{W_p} \sum_{q \in S} G_{\sigma_s}(\|p - q\|) G_{\sigma_r}(|I_p - I_q|) I_q$$

Normalization
Factor



Space Weight

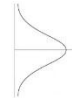


Fig. 4. Bilateral Filtering

- c. Image Histograms: To better comprehend the distribution of pixel intensities over the entire image, we have used image histograms in our research. It's represented as a graph with 255 bins for each pixel value. This specialized examination provides an overview of contrast, brightness, and intensity distribution. It allows us to quickly identify the Background and grey value range. Clipping and Quantization Noise in image values can also be identified right away.

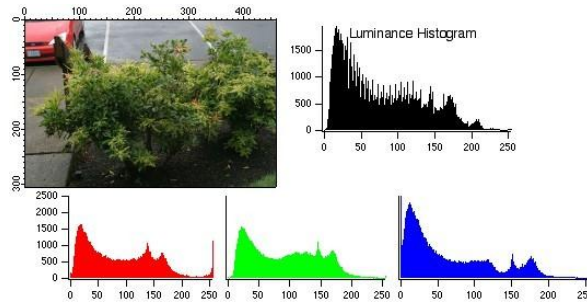


Fig. 5. Image Histograms

C. Models

1. ANN

The Artificial neural network is a widely used training architecture for the classification of images. The traditional approach of ANN starts with converting the image into a grid of pixel values ranging from 0-255. The required object has marginally different values than other parts, thus forming the scope for classifying the difference. The first layer of the network contains a chain of neurons that need one-dimensional input. The flattening of grids (usually multidimensional like 2*2 or 7*7) is necessary. The multiple hidden layers function for better learning. Each hidden or dense layer contains neurons that connect

to every neuron in the previous layer. The value of the connections depends on the weights assigned and the activation function. Every iteration formulates the difference between the actual and predicted output. The back propagation starts after the results, and the weights are changed accordingly. They keep changing till the maximum possible accuracy.

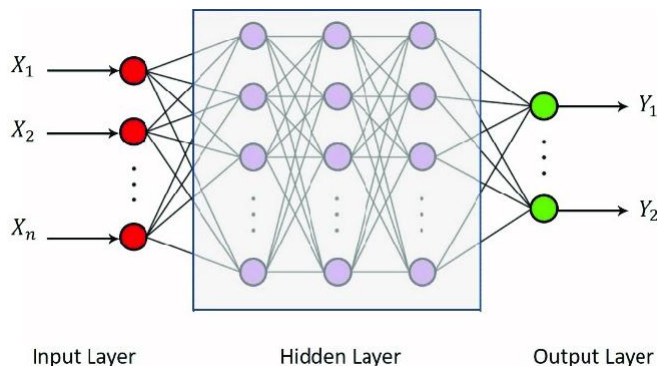


Fig. 6. Pictorial View of ANN

However, this model does have some drawbacks:

- Too much computation- A large-sized complex image may generate millions of neurons in the input layer, which is not computationally efficient
- Sensitive to locality- A dog in an image remains a dog even if it is present at the left, right, or center. The ANN architecture learns the image at a particular location. It leads to inaccuracies for changed positions.

2. CNN Over ANN

The Convolutional Neural Network(CNN) differs from ANN in terms of image partitioning. The ANN learns the entire image at a position while CNN learns individual parts. The change in position of image doesn't affect CNN. It is a significant advantage over ANN. The mechanism of CNN involves three key steps:

a. Convolutional Operation or Filter

b. Activation Function

c. Pooling

d. Dropout Layer

The convolutional filter involves multiplying the image grid with a smaller matrix. For example, if the image grid is 5*7, then it would be multiplied with a 3*3 matrix with sample sizes of 3*3 in the grid. It generates a feature map that has higher values at the cells where our target object is present. The activation function brings nonlinearity to the data. The absence of an activation function makes the network similar to linear regression. It assumes a linear relationship between dependent and independent variables. The real-world data hardly has a linear relationship. For example, a RELU function converts negative values to zero. It eliminates linearity. The pooling layers are responsible for size reduction. It ensures the conversion of the larger grid to a smaller one containing necessary information. Max pooling selects the maximum value from the subset of the grid, while average pooling selects the average of the subset values.

We also added a dropout layer. At each update of the training phase, Dropout works by setting the outgoing edges of hidden units (neurons that make up hidden layers) to 0. This technique provides a computationally simple and highly effective regularization strategy for deep neural networks of all types to prevent overfitting and enhance generalization error.

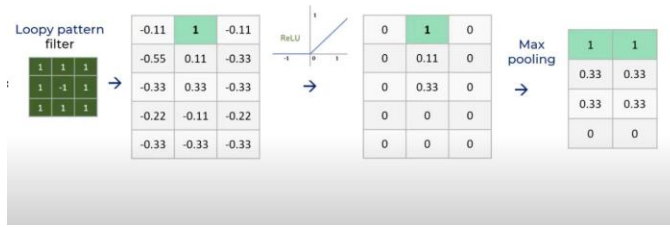


Fig. 7. Different Parts of the model

The different parts of the images get trained through the combination of the above layers. The model learns the entire object image when an aggregated form of already learned partitions passes the layers again. The CNN model functions through multiple sets of Convolutional filters, Activation functions, and Pooling Layers.

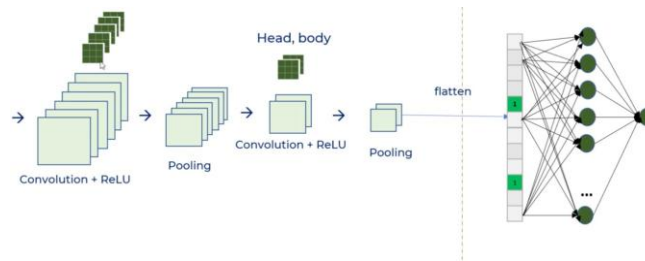


Fig. 8. CNN Model Working

4. PROPOSED METHODOLOGY

Hyperparameter Analysis

Model	Accuracy
ANN	0.8077
CNN	0.9231
CNN (Augmentation Layer)	0.8077
VGG16	0.6154
AlexNet	0.6923

Table 1. Different Models and their accuracies

Deploying and training multiple models was necessary to evaluate performance and choose the right fit for our task. We started by training a simple Artificial Neural Network (ANN) with a few dense layers combined with '*relu*' and '*sigmoid*' activation functions. After training and testing, our model evaluation yielded that the ANN model resulted in an accuracy of 80.77%. However, a loss of 0.35 hinted at inefficiency. We then switched our approach to a Convolution Neural Network (CNN), where we could efficiently perform convolution and pooling compared to ANN. The CNN model resulted in an accuracy of 92.31% over our testing and training data. To shake things up, we augmented our brain images to create a wider variety for the training data and training process and used it over a CNN model again. This CNN model with an augmentation layer yielded an accuracy of 80.77%, which is low compared to the CNN model. However, when averaged, the accuracy is comparatively higher. We wanted to enhance further our understanding of our task and the algorithm that would best fit it; hence, we trained two more models, VGG16 and AlexNet. Both VGG16 and AlexNet resulted in less than 70% accuracy, more specifically 61.54% and 69.23%, respectively.

All in all, *the accuracy for our CNN-based model was the highest, standing at 92.31%*. For the performance measuring of the CNN model, we used a variety of other metrics. Since detecting brain abnormality is a classification task; Hence we needed to evaluate based on classification metrics. Most classification evaluations start with a confusion matrix. A confusion matrix is divided into four segments; True positive, false positives, false negatives, and true negatives. Our convolution neural network had the following confusion matrix:

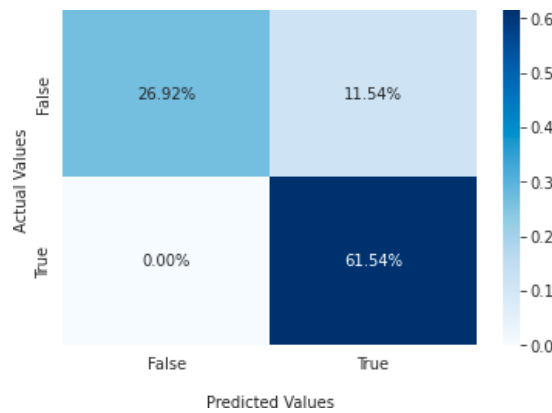


Fig. 8. Confusion Matrix

The confusion matrix above shows that most values fall into the true positive (61.54%). A true positive percentage tells us that most predicted values tend to be similar to the actual value. This in turn tells us that our model is efficient. To support this claim, we can see how the second highest majority is occupied by true negatives (26.92%), which means that most values that are actually 'not abnormal' are also predicted as 'not abnormal.' With the confusion matrix developed, we now resorted to other evaluation metrics, such as:

- Accuracy Score: accuracy score is a measure of the fraction of samples that were predicted correctly. It is given by:

$$Accuracy\ Score = \frac{TP + TN}{TP + TN + FP + FN}$$

$TP + TN + FP + FN$

The accuracy score of our convolutional neural network for brain abnormality detection yielded a score of 92.31%.

- Precision Score: the precision score measures the fraction of predicted positives that were actually positive. The following equation gives this:

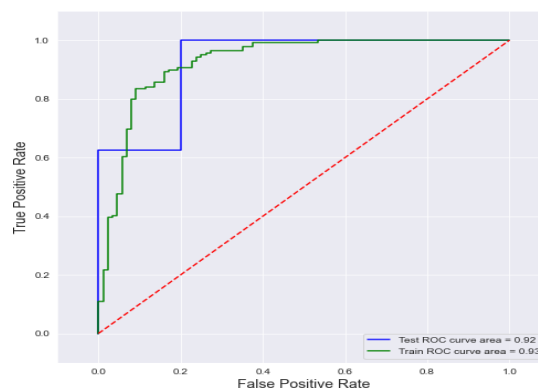


Fig. 10. ROC Curve

As we can see in the figure above, with time, the true positive rate increases exponentially, and on the other hand, the false positive doesn't grow on a significant scale.

- F1 Score: This measure gives us the mean of both recall and precision scores, with higher scores concluding a better model:

- F1 Score =

$$2 \times (\text{Precision} \times \text{Recall})$$

$$\text{Precision Score} =$$

$$\text{TP} / \text{TP} + \text{FP}$$

$$\text{Precision} + \text{Recall}$$

The F1 score of our convolutional neural network for

The Precision score of our convolutional neural network for brain abnormality detection *yielded a score of 78.95%*.

- Recall Score: recall score is a measure of the fraction of positive events that were predicted correctly by the model:

$$\text{Recall Score} =$$

$$\text{TP} / \text{TP} + \text{FN}$$

The recall score of our convolutional neural network for brain abnormality detection *yielded a score of 93.75%*.

Here we can observe that our recall scores are comparatively higher than the precision score. These scores tell us that our model is returning most of the relevant results/predictions. In head of making a more coherent comparison, we used a ROC curve which maps the false positive rate with the true positives rate brain abnormality detection *yielded a score of 85.71%*.

- Jaccard Score: The Jaccard score gives us an idea of how alike the prediction and actual datasets were. We compute a Jaccard score with the following formula:

- Jaccard Score =

$$A \cap B / A \cup B$$

The Jaccard score of our convolutional neural network for brain abnormality detection *yielded a score of 72.22%*.

- Hamming Loss: hamming loss measures the number of labels that were incorrectly predicted over the dataset. In our case, the *hamming loss came out to be 19.23%*.

Comparison

a. Brain-NotBrain Classification

1. MODEL 1

- This model will have the architecture of convolution neural network with convolutional, max pooling, and dense layers.
- The first layer will be a convolutional layer with 32 filters, 3*3 kernel size, with relu as activation.
- The next layer will be a max pooling layer with a pooling size of 2*2

- Next will be another convolutional layer with 64 filters, 3*3 kernel size, and relu activation. Followed by another max pooling layer of pool size 2*2.
- Feature values will be flattened, and they will be passed to a full connected dense network.
- After flattening, the next two layers will be dense layers with number of output nodes as 64 and 10 respectively, with relu activation.
- The final layer will be another dense layer with number of output nodes as 2 with softmax activation to predict whether the input was a brain or not.

2. MODEL 2

Similar to the model 1 used in prediction of abnormal and normal classification below.

b. Abnormal-Normal Classification

1. MODEL 1 (CNN):

- In this model we have taken a Convolutional Neural Network architecture comprising of convolution, pooling, dropout, and dense layers.
- First two layers will be of convolutional layer with 32 and 64 filters respectively, with both having a kernel size of 3*3 and relu as activation.
- Max pooling will be performed in the third layer with a pool size of 2*2, followed by a dropout layer as the fourth layer with 25% of the total nodes being dropped.
- Fifth layer will be a convolutional layer with 64 filters, 3*3 kernel size, and relu activation.
- Sixth layer will be a max pooling layer with a pool size of 2*2, followed by another dropout layer as the seventh layer with 20% dropout rate.
- Next will be another convolutional layer with 128 filters, 3*3 kernel size, and relu activation. Followed by a max pooling layer of pool size 2*2, and a dropout layer of 25%.
- All the matrix values will be flattened using a flattened layer to send the individual values as a single node in a dense neural architecture.
- After flattening, the next layer will be a dense layer with number of output nodes as 64 and relu activation which will again be followed by a dropout layer of 20% dropout rate.
- The final layer will be another dense layer with number of output nodes as 2 with softmax activation, as the architecture would be predicting two classes.

2. MODEL 2 (CNN with Augmentation):

The architecture of model 2 will be similar to model 1, with the addition of an augmentation layer at the beginning. Following are the transformations included in our augmentation layer:

- i. Random translation with 0.2 height and width factor and wrap as the fill mode:

During training, this layer will apply random translations to each image, filling empty space according to the fill mode.

ii. Random flip with horizontal mode:

Depending on the mode parameter, this layer will flip the photos horizontally or vertically. The output will be identical to the input at inference time.

iii. Random rotation with factor of 0.1:

This layer will rotate each image at random, filling empty space according to the fill mode.

iv. Random contrast with a factor of 0.2:

This layer will use a random factor to modify the contrast of an image. During training, the contrast of each channel of each image is modified separately.

v. Random zoom with a factor of 0.1:

This layer will zoom in and out of a picture at random on each axis, filling empty space according to fill mode.

3. MODEL 3 (VGG16):

The architecture used in this model is called VGG16. The input to the first convolutional layer is a 224 * 224 RGB image with a fixed size. A sequence of convolutional layers are being used to process the image, each with a relatively restricted receptive field of size 3*3.

A few of the configurations also utilizes 1*1 convolution filters, which could be conceived as a linear change of the input channels.

The stride of the convolution is always 1 pixel.

Portion of the convolutional layers are succeeded by five max-pooling layers, which perform spatial pooling.

Stride of 2 will be used to max-pool over a 2*2 pixel frame.

Three Fully Connected layers accompany a stack of convolutional layers. The first 2 will always have 4096 channels, while the 3rd will have 1000 channels due to the usage of a 1000-way ILSVRC classification system (one for each class). The last layer would be the soft-max layer. The fully connected levels in all networks are set up in the same way, with each concealed layer having a ReLU activation function.

4. MODEL 4 (AlexNet):

The AlexNet architecture consists of 8 layers with 3 FC layers AND 5 convolutional layers. This architecture is famous for avoiding overlapping as it has 60 million parameters. Approaches used in this model:

i. ReLU Nonlinearity:

Relu is employed instead of a tanh function, which was quite common until then. The benefit of ReLU is noticeable while training our dataset. It has been proven that while training using the CIFAR-10 dataset, compared to CNN with tanh the CNN models using ReLU activation can reach a 25% error six quicker.

ii. Overlapping Pooling:

In CNNs, the outcomes of neighboring interconnected neurons are frequently pooled. However, introducing overlap yielded a 0.5 percent drop in error, suggesting that models with overlapping pooling are more challenging to overfit.

iii. Standardization (Local Response Normalization):

Instead of applying standardization to the entire image, a specific section was selected. This approach enhances the model's overall effectiveness.

The formula behind the size of output image for the next layer:

n-in: Number of input features

n-out: Number of output features
k: convolutional kernel size

p: convolutional padding sizes
s: convolutional stride size

$$n_{out} = \left\lfloor \frac{n_{in} + 2p - k}{s} \right\rfloor + 1$$

5. CONCLUSION

We successfully developed a solution to our problem of classifying an abnormal brain from a normal brain. With the use of Convolutional Neural Network based model we were able to construct a system of classification capabilities with high accuracy and performance. With advance per-processing techniques, labelling and data augmentation we were able to provide the necessary

Brain Abnormality Classification



Fig. 11. The Web App

characteristics to our model. Our final model yielded an accuracy of 92.31%. In order to showcase our model and its working, we were also able to successfully develop a fully managed web-app to classify brain images and abnormalities as it can be seen in the image below:

With properly developed CNN Design, our model can be used to classify brain abnormalities from any image.

REFERENCES

1. Van Hespen, K.M., Zwanenburg, J.J.M., Dankbaar, J.W. et al. An anomaly detection approach to identify chronic brain infarcts on MRI. *SciRep* **11**, 7714 (2021). <https://doi.org/10.1038/s41598-021-87013-4>

2. Baur C, Wiestler B, Muehlau M, Zimmer C, Navab N, Albarqouni S. Modeling Healthy Anatomy with Artificial Intelligence for Unsupervised Anomaly Detection in Brain MRI. *Radiol Artif Intell.* 2021 Feb 17;3(3):e190169. doi: 10.1148/ryai.2021190169. PMID: 34136814; PMCID: PMC8204131.
3. Gao, L., Pan, H., Li, Q. *et al.* Brain medical image diagnosis based on corners with importance-values. *BMC Bioinformatics* **18**, 505 (2017). <https://doi.org/10.1186/s12859-017-1903-6>
4. Shahriar, Sakib & Al-Ali, A. & Osman, Ahmed & Dhou, Salam & Nijim, Mais. (2020). Machine Learning Approaches for EV Charging Behavior: A Review. *IEEE Access.* 8. 168980-168993. 10.1109/ACCESS.2020.3023388.
5. Guizard, Nicolas & Coupé, Pierrick & Fonov, Vladimir & Phd, José & Arnold, Douglas & Collins, Louis. (2015). Rotation-invariant multi-contrast non-local means for MS lesion segmentation.
6. Modeling Healthy Anatomy with Artificial Intelligence for Unsupervised Anomaly Detection in Brain MRI ' by Christoph Baur, Benedikt Wiestler, Mark Muehlau, Claus Zimmer, Nassir Navab and Shadi Albarqouni
7. Wavemetrics." *I g o r P r o f r o m W a v e M e t r i c s* , https://www.wavemetrics.com/products/igorpro/imageprocessing/_imagetransforms/histmodification.
8. "Python: Bilateral Filtering." *GeeksforGeeks*, 31 Oct. 2021, <https://www.geeksforgeeks.org/python-bilateral-filtering/>.
9. Grossi, Enzo & Buscema, Massimo. (2008). Introduction to artificial neural networks. *European journal of gastroenterology & hepatology.* 19. 1046-54. 10.1097/MEG.0b013e3282f198a0.
10. Simonyan, Karen & Zisserman, Andrew. (2014). Very Deep Convolutional Networks for Large-Scale Image Recognition. arXiv 1409.1556.
11. K. Lee, S. H. Sung, D. -h. Kim and S. -h. Park, "Verification of Normalization Effects Through Comparison of CNN Models," 2019 International Conference on Multimedia Analysis and Pattern Recognition (MAPR), 2019, pp. 1-5, doi: 10.1109/MAPR.2019.8743531.
12. Hyperspectral Remote Sensing Image Classification Based on Maximum Overlap Pooling Convolutional Neural Network - Scientific Figure on ResearchGate. Available from: https://www.researchgate.net/figure/Maximum-overlap-pooling-CNN-parameter-table_tbl4_328468285 [accessed 22 Jan, 2022]
13. Susmaga R. (2004) Confusion Matrix Visualization. In: Kłopotek M.A., Wierzchoń S.T., Trojanowski K. (eds) *Intelligent Information Processing and Web Mining. Advances in Soft Computing*, vol 25. Springer, Berlin, Heidelberg. https://doi.org/10.1007/978-3-540-39985-8_12
14. H .Ide and T. Kurita, "Improvement of learning for CNN with ReLU activation by sparse regularization," 2017 International Joint Conference on Neural Networks (IJCNN), 2017, pp. 2684-2691, doi: 10.1109/IJCNN.2017.7966185.
15. Han J., Moraga C. (1995) The influence of the sigmoid function parameters on the speed of backpropagation learning. In: Mira J., Sandoval F. (eds) *From Natural to Artificial Neural Computation. IWANN 1995. Lecture Notes in Computer Science*, vol 930. Springer, Berlin, Heidelberg. https://doi.org/10.1007/3-540-59497-3_175